A 6.8μW AFE for Ear EEG Recording with Simultaneous Impedance Measurement for Motion Artifact Cancellation

Aviral Pandey[1], Sina Faraji Alamouti[1], Justin Doong[1], Ryan Kaveh[1], Cem Yalcin[1], Mohammad Meraj Ghanbari[1], and Rikky Muller[1,2]

[1]University of California, Berkeley, [2]Chan-Zuckerberg Biohub

Wearable electroencephalography (EEG) systems can monitor neurological activity, enable new brain-computer interfaces and help users communicate with assistive devices. To facilitate ambulatory EEG recording, recent work has incorporated dry electrodes into wearable headsets and earbuds [1,2]. Dry electrodes have superior ease-of-use over wet electrodes that require abrasive skin preparation. However, due to their high electrode-skin impedance (ESI), dry electrode wearables are susceptible to motion artifacts.

This work uses the dry Ag in-ear electrodes (Ear EEG) [1] pictured in Fig. 1, with *in situ* ESI measurements shown in the bottom right. Motion at the electrode induces variation of the ESI that couples artifacts into the EEG recording. To track changes in ESI, impedance (Z) and EEG can be measured simultaneously from a pair of shared electrodes by driving a current, modulated at the drive frequency (f_z=500Hz-2kHz), outside of the EEG band (1-100Hz). The resulting voltage is proportional to the ESI at f_z. Although the ESI is frequency dependent, motion artifacts cause broadband ESI shifts due to the capacitive nature of the electrode at the frequencies of interest. As a result, the ESI variations at f_z are correlated with those in the EEG band, and the frequency separation allows their concurrent acquisition through an analog front end (AFE). Simultaneous and continuous measurement of EEG and ESI on each electrode enables backend removal, thus reducing the impact of motion artifacts [3]. Prior art has integrated EEG and Z together on-chip for measurement from different wet electrodes [4], and simultaneously from the same wet electrodes [3]. Dry electrodes have orders of magnitude higher ESI than wet electrodes, making it critical to minimize the output current noise of the Z-driver circuit, which can induce voltage noise into the EEG band. This work co-designs a Z-driver and AFE to simultaneously measure ESI and EEG with minimal impact on the EEG noise floor.

To measure ESI, a square wave current (I_Z) is driven on the input at f_z (Fig. 1). Since I_Z terminates on the ESI, the sum of the resulting voltage, the EEG (<1mV) and the motion artifacts (~mVs) sets the full scale. The dry Ear EEG ESI averages 100kΩ across the f_z range, but can be as high as 1MΩ. Since the smallest current that can reliably be driven is on the order of 10nA, an AFE full-scale of 20mV is required. To resolve EEG signals, the AFE, inclusive of the current noise of the Z-driver terminating on the ESI, should have an input referred noise about 1μV_{rms}. In meeting the required noise floor, the AFE also meets the required bandwidth for impedance measurement, enabling simultaneous readout without the power and area penalty of a secondary signal path used by prior art.

A 1024x oversampled 2nd order Continuous Time Delta Sigma (CTΔΣ) ADC (Fig. 1) is chosen to digitize EEG and ESI. Single bit quantization is chosen for its simplicity and superior linearity. To allow complex demodulation of impedance currents up to 2kHz, the 1MS/s output bitstream is filtered and decimated to an intermediate frequency of 8kS/s on an FPGA. Here, the I and Q components of I_z are demodulated to measure the complex ESI (Z_I and Z_Q). EEG, Z_I and Z_Q are further decimated to 1kS/s. Fig. 2 shows the circuit diagram of the AFE consisting of the AC-coupled Z-driver and the CTΔΣ ADC. A 6-bit DAC and mixed signal servo loop removes electrode DC offset (EDO) across a 200mV range. The ADC employs a Gm-C integrator for each stage with transistors biased in subthreshold for noise and power efficiency. The current reuse G_{m1} is chopped at 8kHz to mitigate flicker noise and allow capacitive summing of feedback signals. Since chopping reduces the input impedance of the ADC, optional pre-charge-based impedance boosting [5] increases the input impedance from 20MΩ to 230MΩ. To remove the need for excess loop delay compensation and to prevent chopping from folding quantization noise, the 1-bit ΔΣ feedback DAC is implemented as a return-to-zero (RZ) DAC. The chopping is timed to change phase while the feedback DAC is inactive, preventing the chopper from sampling residual quantization noise. The ADC achieves a maximum SNDR of 76.7dB and a noise floor of 62nV/√Hz with grounded inputs (Fig. 3a-b). When terminated by the average ESI (100kΩ), the noise floor rises to 140nV/√Hz, and activating the Z-driver has no effect (Fig. 3d).

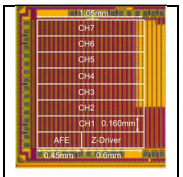

Die micrograph.

The schematic of the Z-driver is shown in Fig. 2. To allow the electrodes to be biased at ground, it is AC-coupled using two 50pF on-chip capacitors. Less than 1% |Z| error requires a minimum SNR (μ/σ) of 25dB. To achieve this over an ESI range of 1kΩ-1MΩ, currents between 14-42nApp are used. The Z-driver uses a regulated differential current source with resistive degeneration to avoid flicker noise from current mirrors. To further eliminate flicker noise, the regulating amplifiers are chopped and 4-bit resistive DACs set per-channel reference voltages V_{bn} and V_{bp}. Driving 42nApp induces less than 60fA/√Hz of output current noise density over the EEG band. High gain regulating amplifiers raise the output impedance of the Z driver to >1GΩ to avoid reducing the input impedance of the channel. The Z readout achieves the required SNR for resistors across the ESI range (Fig. 4a-b) and achieves 7.2Ω/√Hz (Fig. 4c) when driving 34nApp, corresponding to 122nV/√Hz at f_z. Due to noise shaping from the CTΔΣ, the noise floor at f_z is slightly higher than in the EEG band. Fig. 4d shows impedance measurements of three electrode models.

Simultaneous EEG and ESI measurements were made *in vivo* using dry electrode Ear EEG (Fig. 1). In accordance with UC Berkeley's Institutional Review Board (CPHS protocol ID: 2018-09-11395), sense and reference electrodes were placed in ear while a ground electrode was attached behind the ear. The user opened and closed their eyes for one-minute intervals to modulate alpha band (8-12 Hz) activity. Fig. 5a shows recordings with motion artifacts created by tapping on the electrodes and Fig. 5b shows the corresponding EEG time-frequency spectrogram. A 4th order least mean squares filter with the ESI as the noise-reference signal cancels motion artifacts from the EEG in postprocessing (Fig. 5c) showing 19dB artifact amplitude reduction. Fig. 5d shows the corresponding spectrogram with significantly reduced spectral interference in the alpha band.

The 8 channels occupy 1.344mm^2 in TSMC's 28nm CMOS process. The AFE consumes 6.8μW/channel and 5.6μW/channel with and without the Z-driver respectively. Backend digital signal processing was implemented on an FPGA as shown in Fig. 2 and consumes 15μW/channel when synthesized. Fig. 6 shows the performance summary and comparison with recent state-of-the-art AFEs for biopotential recording compatible with dry electrodes, including one with simultaneous Z [3]. The shared signal path AFE in this work exhibits comparable noise and power performance to EEG AFEs and the lowest NEF and PEF among prior art with >1mVpp input range. The AFE also has lower power and area than prior art that integrates EEG and Z. To the authors' knowledge, this work is the first to demonstrate *in vivo* motion artifact cancellation by simultaneously recording EEG and Z on dry electrodes.

Acknowledgements:

The authors thank Prof. Ana C. Arias, the sponsors of BWRC, and TSMC for chip fabrication.

References:

[1] R. Kaveh *et al*., "Wireless User-Generic Ear EEG," *TBioCAS*, Aug 2020.

[2] J. Lee *et al*., "A 0.8-V 82.9-μW In-Ear BCI Controller IC with 8.8 PEF EEG Instrumentation Amplifier and Wireless BAN Transceiver," *JSSC*, Apr. 2019.

[3] N. Van Helleputte *et al*., "345 μW Multi-Sensor Biomedical SoC With Bio-Impedance, 3-Channel ECG, Motion Artifact Reduction, and Integrated DSP," *JSSC*, Jan. 2015.

[4] J. Xu *et al*., "A 665μW Silicon Photomultiplier-Based NIRS/EEG/EIT Monitoring ASIC for Wearable Functional Brain Imaging," *TBioCAS*, Dec. 2018.

[5] H. Chandrakumar *et al*., "A 15.2-ENOB 5-kHz BW 4.5 μW Chopped CT ΔΣ-ADC for Artifact-Tolerant Neural Recording Front Ends," *JSSC*, Dec. 2018.

[6] C. Pochet *et al*. "A 400mVpp 92.3dB-SNDR 1kHz-BW 2nd-Order VCO-Based ExG-to-Digital Front-End Using a Multiphase Gated-Inverted Ring-Oscillator Quantizer," *ISSCC*, Feb. 2021.

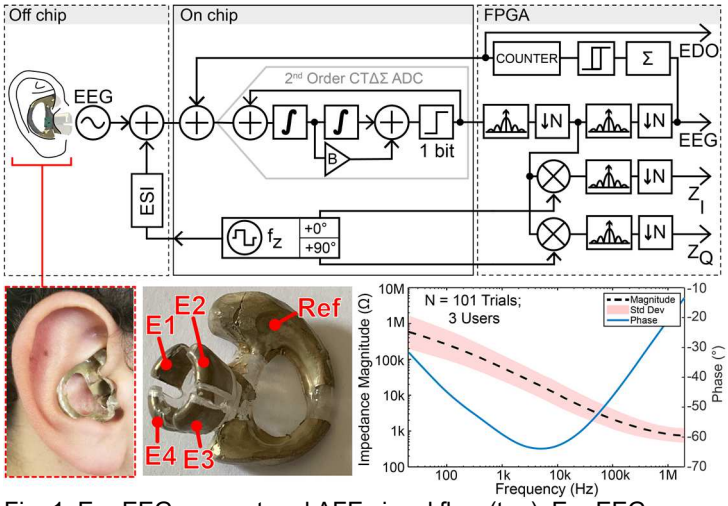

Fig. 1. Ear EEG concept and AFE signal flow (top); Ear EEG earpiece with dry Ag electrodes from [1] (bottom left); *in situ* electrode-skin impedance spectrum showing mean and standard deviation across 101 measurements in 3 users (bottom right).

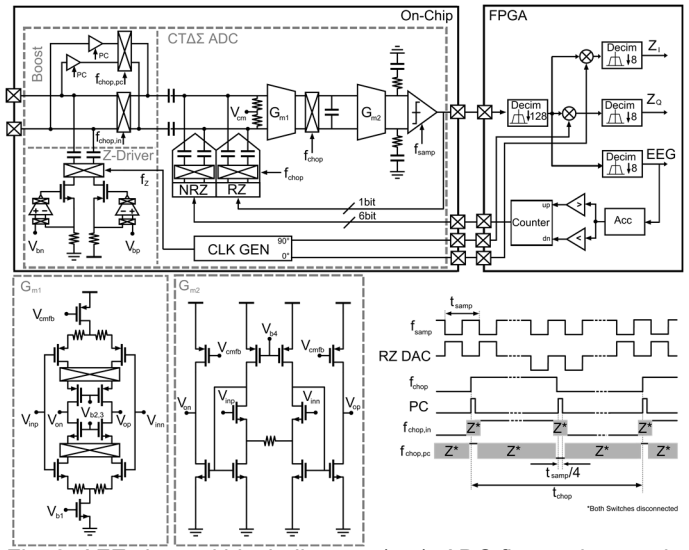

Fig. 2. AFE channel block diagram (top); ADC first and second stage integrator OTAs (bottom left); timing diagram (bottom right).

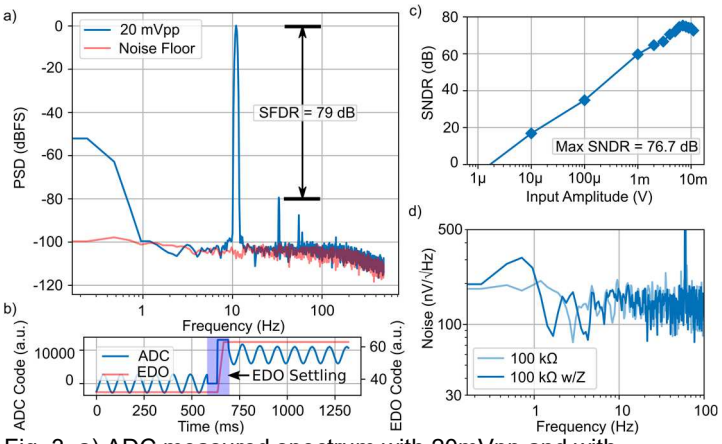

Fig. 3. a) ADC measured spectrum with 20mVpp and with grounded inputs; b) EDO loop settling behavior with 100mV step in the input DC and a 10mVpp sinusoid; c) SNDR vs input amplitude; d) input noise across the EEG band with and without Z measurement active for 100kΩ input resistance.

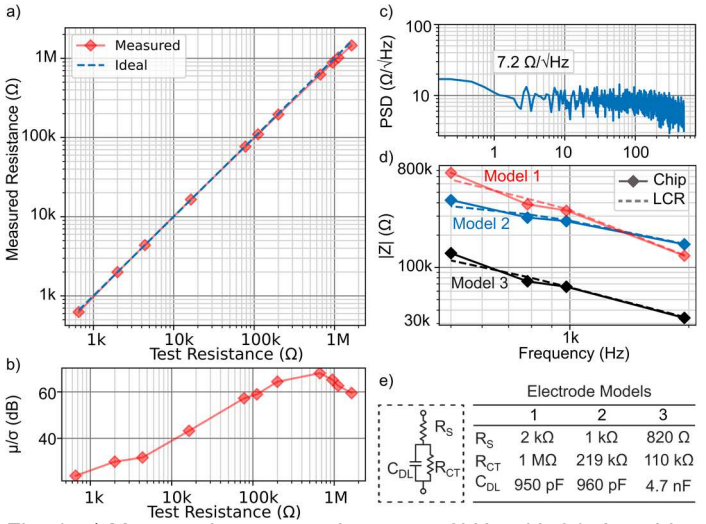

Fig. 4. a) Measured vs. test resistance at 2kHz with 34nApp drive current; b) SNR across resistance; c) Z readout IRN; d) impedance measurements of 3 electrode models compared to an LCR meter; e) parameters for the electrode models used in d).

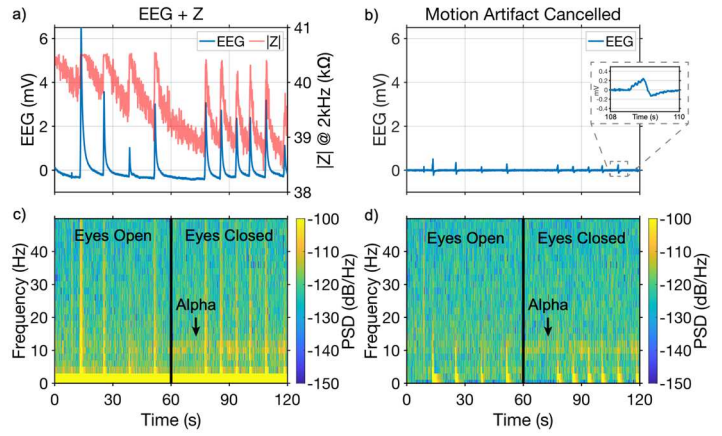

Fig. 5. a) Simultaneous Ear EEG and ESI measurements in the presence of motion artifacts; b) corresponding EEG spectrogram showing alpha band contaminated; c) EEG showing 19dB reduction in artifact amplitude after motion artifact cancellation via 4th order least mean squares adaptive filter; d) corresponding spectrogram with clearly visible alpha modulation.

	Reference	ISSCC '21 [6]	JSSC '19 [2]	TBioCAS '18 [4]	JSSC '15 [3]	This Work
System	Biopotential	ECG	EEG	EEG	ECG	EEG
	Simultaneous Z	No	No	Diff. Elec.	Same Elec.	Same Elec.
	Technology (nm)	65	65	180	180	28
	Area/Ch (mm²)	0.075	4*	2.7*	5.5*	0.168
	Supply (V)	1.2	0.8	1.2	1.2	1
Biopotential AFE	Architecture	2nd Order VCO	SAR	2nd Order DSM	2nd Order DSM	2nd Order CTDSM
	Power/Ch (μW)	5.8	5	43	31	5.6
	Bandwidth (Hz)	1000	1000	200	150	100
	DR (dB)	92.3	57*	78.4*	84.3	81.4
	CMRR (dB)	89	95	100	>110	88
	60Hz Input Z (MΩ)	60	1000	720	>500	230
	Peak Input (mVpp)	400	0.8	40	30	20
	EDO Tolerance (mV)	N/A†	700	600	800	200
	Grounded IRN (nV/√Hz)	110	40*	120	52	62
	NEF/PEF	9.89*/117.3*	3.84/11.8	29.3*/1030*	10.8*/139*	7.16/51.3
Impedance	Z Power/Ch (μW)	-	-	45	19*	1.2
	Z Current Level (μApp)	-	-	10 - 200	27 - 117	0.014 - 0.042
	Z IRN @ f_Z (nV/√Hz)	-	-	120*	94	122
	Z Noise (Ω/√Hz)	-	-	0.003	0.0098	7.2

*Estimated
†ADC quantizes EDO

Fig. 6. Table of comparison of biopotential and impedance digitizing AFEs.